Acta Crystallographica Section B
Structural Science
ISSN 0108-7681

An X-ray powder diffraction study of the spin-crossover transition and structure of bis(2,6-dipyrazol-1-ylpyrazine)iron(II) perchlorate

Victoria A. Money,[a] Ivana Radosavljevic Evans,[a] Jerome Elhaïk,[b] Malcolm A. Halcrow[b] and Judith A. K. Howard[a]*

[a]Chemistry Department, Durham University, South Road, Durham DH1 3LE, UK, and [b]Department of Chemistry, University of Leeds, Leeds LS2 9IT, UK

Correspondence e-mail: j.a.k.howard@durham.ac.uk

Received 23 September 2003
Accepted 3 December 2003

The crystal structure of the iron(II) spin-crossover compound $[Fe(C_{10}H_8N_6)_2](ClO_4)_2$ in the high-spin state has been solved from powder X-ray diffraction data using the *DASH* program and refined using Rietveld refinement. The thermal spin transition has been monitored by following the change in unit-cell parameters with temperature. The title compound has been found to undergo a crystallographic phase change, involving a doubling of the crystallographic *a* axis, on undergoing the spin transition.

1. Introduction

The spin-crossover phenomenon in an iron(II) compound was first reported by Baker & Bobonich (1964). Since then, much attention has been focused on these materials because of their potential for use in applications such as molecular switches, display devices and information storage, as well as their interest as model compounds for biological and geological systems (Gütlich *et al.*, 1994, 2000). Most reported examples have been of organometallic systems, in which the Fe atom is bound to six N atoms. These materials are of special interest crystallographically as the spin transition gives rise to large changes in the structure of the complexes in the crystalline state. Crystallographic techniques can be used to closely follow the course of the spin transition with temperature, pressure and light irradiation. On going from the high- to the low-spin state, there is a dramatic decrease in the lengths of the metal–ligand bonds, which is caused by the reduction in effective radius of the metal ion; for $[FeN_6]$ systems, this decrease is $\sim$0.2 Å. The transition is also accompanied by a change in the molecular conformation to a less distorted octahedral geometry. The diminution in metal–ligand bond length leads to a decrease in the size of the coordination polyhedron and in the unit-cell volume. In cases where there is a large degree of hysteresis in the transition, a necessary property for many of the applications mentioned above, the transition is frequently associated with a change in crystallographic space group. A thermochromic effect in the crystal is often observed, with the crystals becoming darker on going from the high- to the low-spin state.

Previous work on iron(II) compounds of ligands based on the 2,6-dipyrazolpyridine ligand has enabled us to obtain spin-crossover materials in which the transition occurs at a relatively high temperature, is abrupt and shows hysteresis (Holland *et al.*, 2001, 2002; Money *et al.*, 2003). One of the most interesting features of spin-crossover materials is the so-called

© 2004 International Union of Crystallography
Printed in Great Britain – all rights reserved

Table 1
Crystallographic data and *GSAS* refinement details for the room-temperature structure of $[Fe(C_{10}H_8N_6)_2](ClO_4)_2$.

Chemical formula	$[Fe(C_{10}H_8N_6)_2](ClO_4)_2$
Radiation type	1.54056 Å (Cu $K\alpha_1$)
2θ range (°)	5–50
2θ step size (°)	0.0144
Space group	$P2_1$
a (Å)	8.4538 (8)
b (Å)	8.4462 (7)
c (Å)	19.436 (2)
β (°)	90.450 (5)
Volume (Å^3)	1387.7 (2)
Z	2
Number of degrees of freedom	18
Number of Z matrices	3
Number of Bragg reflections	280
Number of profile points	3011
Number of restraints	94
Number of observations	3105
Number of refined parameters	152
R_p	0.030
wR_p	0.047
R_{F^2}	0.079

LIESST effect (light induced excited spin state trapping). Irradiation of a crystal at low temperature with an intense light source causes the formation of a metastable high-spin state. Despite the intense interest in this phenomenon, structural information about the metastable state is very rare; as far as we are aware, only three crystallographic studies of this excited state have been reported (Kusz *et al.*, 2001; Marchivie *et al.*, 2002; Money *et al.*, 2003).

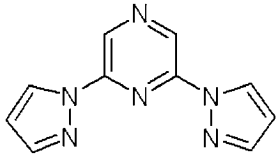

In recent years, significant advances have been made in the area of structure solution of molecular solids from powder diffraction, largely owing to development of direct space methods, such as simulated annealing, Monte Carlo and genetic algorithm techniques (Harris, 2002). In these methods, trial structures are generated independently of the observed diffraction data and their correctness is evaluated using appropriate agreement factors based on the comparison between the calculated and the experimental powder patterns. For molecular structures, the complexity of the crystallographic problem is determined by the number of torsion angles in a molecule and the number of independent molecules in the structure.

2. Experimental

$[Fe(C_{10}H_8N_6)_2](ClO_4)_2$ was synthesized using literature methods (Elhaïk *et al.*, 2003); however, we were unable to grow single crystals of the unsolvated compound, although small crystals of the solvated complex $[Fe(C_{10}H_8N_6)_2](ClO_4)_2\cdot MeCN$ were obtained. We have previously published tentative unit cells for the high-spin state of $[Fe(C_{10}H_8N_6)_2](ClO_4)_2$, obtained from powder data and the magnetic curves of this and the analogous BF_4 salt. $[Fe(C_{10}H_8N_6)_2](ClO_4)_2$ undergoes an abrupt transition at 208 K, with a small hysteresis loop, and has also been shown to exhibit LIESST behaviour (Money *et al.*, 2002).

All powder X-ray diffraction data were collected on a Bruker *D*8 diffractometer equipped with an mBraun linear PSD and a Ge(111) incident-beam monochromator, using Cu $K\alpha_1$ radiation. Room-temperature data were collected in the capillary mode. The sample was lightly ground, sieved and loaded into a capillary with a 0.5 mm diameter. The capillary was filled with polycrystalline sample up to ~3.5 cm in length and sealed; the capillary was kept spinning throughout the data collection. Patterns were recorded in the 2θ range between 4 and 90°, in 0.0144° steps, with a step time of 7 s. Nine powder patterns were collected and summed, resulting in an overall collection time of 105 h.

Variable-temperature data were collected in the flat-plate mode using an Oxford Cryosystems PHENIX helium cryostat (Money *et al.*, 2003). The powder was sieved onto an Al sample holder until an even coverage and a smooth surface were achieved. A total of 16 patterns were collected between 290 and 130 K, with a cooling rate of 17 K h^{-1}. Patterns were collected in the 2θ range between 5 and 37°, in 0.0144° steps, using a counting time of 0.85 s step^{-1}, resulting in a collection time of 30 min per temperature range. Experimental details are given in Table 1.[1]

3. Results and discussion

3.1. Indexing and structure solution

The room-temperature powder diffraction data were indexed using 20 peaks between 5 and 50° 2θ, with an in-house modification of the indexing program of Visser (1969), to give an orthorhombic unit cell of a = 8.44, b = 8.45 and c = 19.4 Å. Examination of related compounds led us to believe that this cell was most likely to be monoclinic, with a β angle close to 90°. Inspection of the systematic absences suggested that the possible space groups were $P2_1$ or $P2_1/m$. Similar compounds have previously been reported to crystallize in the space group $P2_1$ and so it might have been expected that $[Fe(C_{10}H_8N_6)_2](ClO_4)_2$ would have similar packing. This prediction was supported by experimental results. Second-harmonic generation measurements gave a positive non-linear optical response, demonstrating that the material must be non-centrosymmetric, and the space group was therefore assigned to be $P2_1$.

The structure solution was performed by simulated annealing in *DASH* (Cambridge Crystallographic Data Centre, 2002). Three Z matrices were used, *viz.* one for each of the two unique ClO_4^- anions and one for the cation. The Z

[1] Supplementary data for this paper are available from the IUCr electronic archives (Reference: BM5003). Services for accessing these data are described at the back of the journal.

matrix for the $[Fe(C_{10}H_8N_6)_2]^{2+}$ cation was based on the molecular structure of the related $[Fe(C_{11}H_9N_5)_2]^{2+}$ molecule and was treated as a rigid body during simulated annealing. 50 cycles of ten million moves were performed, giving a best solution with χ^2 of 40.88 after 8305500 moves. Visual inspection of the possible solutions showed that the solution with the lowest χ^2 value was indeed that which made the most chemical and physical sense, and this solution was chosen to be taken forward for refinement.

3.2. Refinement

Before refinement could commence, a set of suitable restraints had to be introduced, and these were found through searches for appropriate fragments in the Cambridge Structural Database (CSD; Allen, 2002).

Magnetic measurements have confirmed that the material is fully high-spin at 290 K (Elhaïk *et al.*, 2003). A CSD search for iron(II) centres bound to six N atoms reveals the existence of two peaks in the histogram, one centred around 1.95 Å, which is due to low-spin iron(II) centres, and the second centred around 2.2 Å, which is due to high-spin iron(II) centres. A CSD search was therefore performed to look for high-spin iron bound to six N atoms, and the mean of the six Fe—N bond lengths was calculated. In order to ensure that only high-spin centres were taken into consideration, the search was limited to bond lengths between 2.0 and 2.3 Å. This search gave 121 fragments, with a mean Fe—N bond length of 2.170 Å. The Fe—N bonds were therefore restrained to 2.17 (1) Å in the refinement of the title compound.

The perchlorate bond angles were restrained to 109.0 (1)°. A search of the CSD showed that the mean Cl—O bond length in perchlorate is 1.39 Å, and the bonds in the title compound were therefore restrained to 1.39 (1) Å.

It was necessary to restrain the aromatic rings within the ligand to be planar. To this end, planar restraints were introduced for ring 1 (N1/N2/C1–C3), ring 2 (C4/C5/N11/C7/C8/N3), ring 3 (C9–C11/N4/N5), ring 4 (N6/N7/C12–C14), ring 5 (N8/C15/C16/N12/C18/C19) and ring 6 (N9/N10/C20–C22).

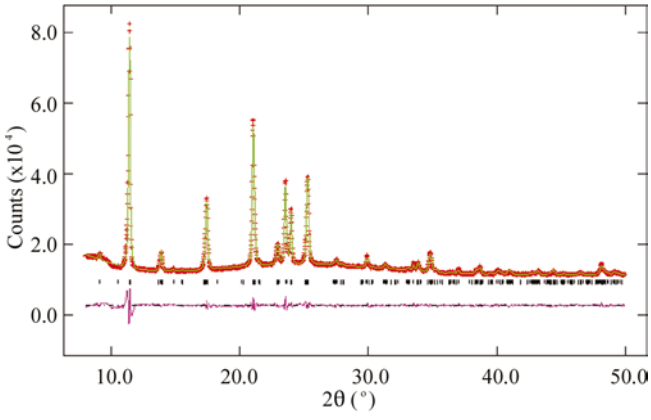

Figure 1
The final Rietveld plot for $[Fe(C_{10}H_8N_6)_2](ClO_4)_2$ (observed: red; calculated: green; difference: pink).

Bond lengths within the rings were also restrained. A CSD search for pyrazole bound to one C atom through one of the N atoms yielded 129 hits and allowed restraints to be applied to the bonds within the pyrazole rings. The N—N bonds were restrained to 1.36 (1) Å and the pyrazole N—C bonds to 1.34 (1) Å; finally, the pyrazole C—C bonds were restrained to 1.37 (1) Å. A similar database search, performed for pyrazine bound to a transition metal through one of the N atoms, gave 228 hits. Pyrazine C—C bonds were restrained to 1.38 (1) Å and C—N bonds to 1.33 (1) Å. Bond angles within five-membered rings were restrained to 108.0 (1)° and those within six-membered rings to 120.0 (1)°.

Rietveld (1969) refinement was performed with the *GSAS* suite (Larson & von Dreele, 1994) on the solution imported from *DASH*. The displacement parameters of all non-H atoms were refined isotropically and were constrained to be the same for each element, with only one parameter refined for carbon and nitrogen. The background level of the experimental powder pattern was fitted using a Chebyshev polynomial function. A total of 152 parameters were refined: four unit-cell parameters, a zero point, a histogram scale factor, four profile parameters, nine terms of the Chebyshev background function, 129 atomic positional parameters and four isotropic displacement parameters.

The final agreement factors obtained were $R_p = 0.030$, $wR_p = 0.047$ and $R_{F^2} = 0.079$ (see Fig. 1).

3.3. Description of the structure

$[Fe(C_{10}H_8N_6)_2](ClO_4)_2$ crystallizes in the monoclinic space group $P2_1$; the asymmetric unit consists of one cation and two counter-ions (Fig. 2) and the compound is isostructural with $[Fe(C_{11}H_9N_5)_2](BF_4)_2$ (Holland *et al.*, 2002; Money *et al.*, 2003). The iron(II) ion has a distorted octahedral geometry and is bound equatorially to two ligands through three of the ligands' six N atoms. There are four bonds from N atoms in the pyrazole rings and two from N atoms in the pyrazine rings. The shortest bonds are formed between the central pyrazine rings and the iron ions and lie along the crystallographic *c* axis. The Fe—$N_{pyrazine}$ bonds lie at ∼45° to the *a* and *b* axes.

It is well known that intermolecular bonding plays an important role in the transmission of the spin transition through the material and in this way can be crucial in deter-

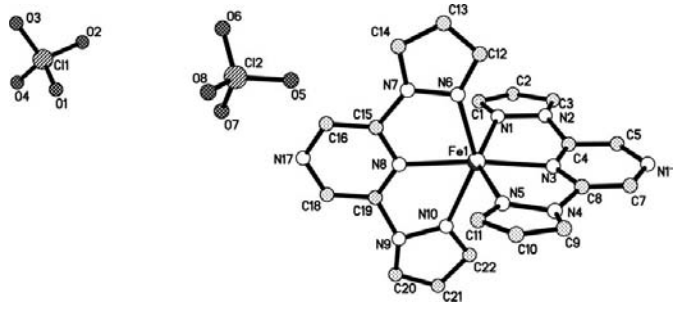

Figure 2
The crystal structure of $[Fe(C_{10}H_8N_6)_2](ClO_4)_2$, showing the atom-numbering scheme. H atoms have been omitted for clarity.

mining the course of the transition, *i.e.* whether it is smooth or discontinuous, abrupt or gradual. In common with other materials in this series, $[Fe(C_{10}H_8N_6)_2](ClO_4)_2$ exhibits π–π interactions between the pyrazole rings of the ligands, which lead to the formation of chains of cations linked along the *a* axis (Fig. 3). Adjacent chains are linked *via* weak hydrogen bonds between the CH groups of the ligands and the O atoms of the percholorate anions. It is interesting to note that the substitution of pyrazine for the pyridine ring present in $[Fe(C_{11}H_9N_5)_2](BF_4)_2$ has had no effect on the packing of the crystal and very little effect on the intermolecular bonding. It is probably for these reasons that the two materials have the same type of spin transition, being very abrupt and showing a small amount of hysteresis. The effect of the pyrazine ring on the ligand field energy is likely to be responsible for the lower temperature transition for the title compound.

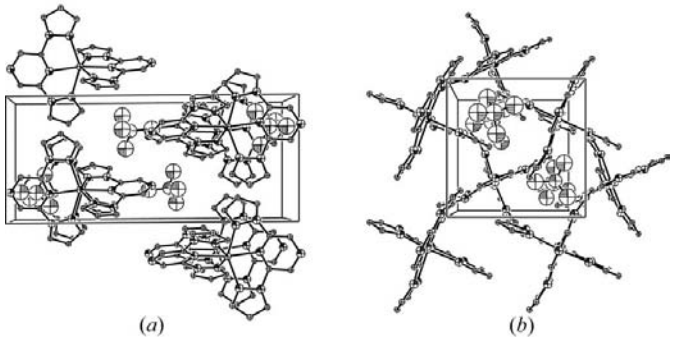

Figure 3
The packing in $[Fe(C_{10}H_8N_6)_2](ClO_4)_2$ (*a*) normal to 010 and (*b*) normal to 001. H atoms have been omitted for clarity.

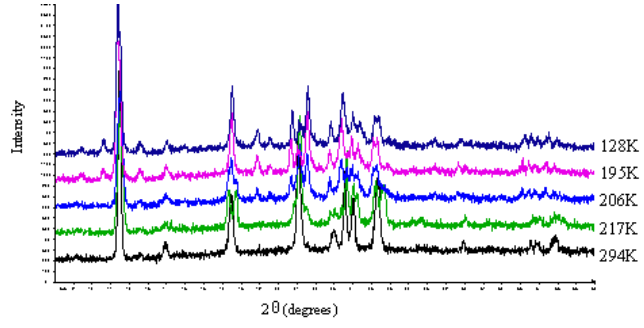

Figure 4
The evolution of the powder diffraction pattern of $[Fe(C_{10}H_8N_6)_2](ClO_4)_2$ with temperature (only selected temperatures are plotted for clarity).

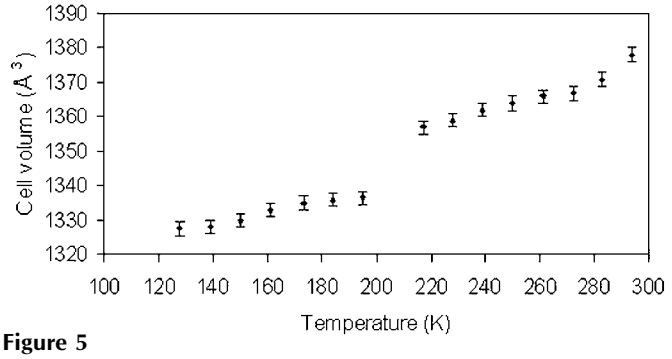

Figure 5
Variation in unit-cell volume with temperature on cooling for $[Fe(C_{10}H_8N_6)_2](ClO_4)_2$. Values recorded in the low spin state, below 195 K, have been halved for clarity

3.4. Variable-temperature data analysis

The evolution of the diffraction pattern of $[Fe(C_{10}H_8N_6)_2](ClO_4)_2$ with temperature is shown in Fig. 4 (only selected temperatures are plotted for clarity). Fig. 4 suggests that a phase transition takes place between 217 and 195 K, and this result is in good agreement with the magnetic data. Variable-temperature data analysis in the observed range was performed using two different approaches. Starting from room temperature, the first eight patterns were analysed using a structural model, by Rietveld refinement, where the cell parameters and an overall temperature factor were refined in addition to the sample displacement, profile and background coefficients. The powder pattern collected at 195 K, which is representative of the low-spin structure, was indexed to a unit cell with $a = 16.571$ (3), $b = 8.568$ (1), $c = 18.839$ (4) Å, $\beta = 92.33$ (1)° and $V = 2673$ (2) Å^3. This unit cell appears to have twice the volume of the room-temperature phase, and the dimensions correspond to a doubling of the crystallographic *a* axis. With this unit-cell volume and the expected symmetry, the low-spin structure of $[Fe(C_{10}H_8N_6)_2](ClO_4)_2$ would consist of six crystallographically independent fragments, thus rendering structure solution very difficult given the current computational facilities. The analysis of the low-spin data was therefore performed using Pawley (1981) fitting, where the unit-cell, sample-displacement, profile and background parameters were refined. At 206 K, the data set was found to be a mixture of the high- and low-spin phases. The temperature dependence of the unit-cell volume of $[Fe(C_{10}H_8N_6)_2](ClO_4)_2$ is shown in Fig. 5 (for ease of comparison, the unit-cell volumes of the low-spin phases below 195 K have been halved in this plot). The discontinuity in the unit-cell volume is in good agreement with the change in the magnetic curve.

This result is particularly interesting as the title compound is the first in the series that we have been studying that has been shown to undergo this type of structural phase change on passing through the spin transition.

The authors would like to thank the EPSRC for two studentships (VAM and JE) and a senior research fellowship (JAKH) and the Royal Society for financial support (MAH), as well as Dr Marek Szablewski of the Department of Physics, University of Durham, for performing the SHG experiments.

References

Allen, F. H. (2002). *Acta Cryst.*, B**58**, 380–388.
Baker, W. A. & Bobonich, H. M. (1964). *Inorg. Chem.* **3**, 1184–1188.

Cambridge Crystallographic Data Centre (2002). *DASH*. Version 2.1. Cambridge Crystallographic Data Centre, 12 Union Road, Cambridge CB2 1EZ, UK.
Elhaïk, J., Money, V. A., Barrett, S. A., Kilner, C. A., Evans, I. R. & Halcrow, M. A. (2003). *Dalton Discuss.* pp. 2053–2060.
Gütlich, P., Garcia, Y. & Goodwin, H. A. (2000). *Chem. Soc. Rev.* **29**, 419–427.
Gütlich, P., Hauser, A. & Spiering, H. (1994). *Angew. Chem. Int. Ed. Engl.* **33**, 2024–2054.
Harris, K. D. M. (2002). *Curr. Opin. Solid State Mater Sci.* **6**, 125–130.
Holland, J. M., McAllister, J. A., Kilner, C. A., Thornton-Pett, M., Bridgeman, A. J. & Halcrow, M. A. (2002). *J. Chem. Soc. Dalton Trans.* pp. 548–554.
Holland, J. M., McAllister, J. A., Lu, Z., Kilner, C. A., Thornton-Pett, M. & Halcrow, M. A. (2001). *Chem. Commun.* pp. 577–578.
Kusz, J., Spiering, H. & Gütlich, P. (2001). *J. Appl. Cryst.* **34**, 229–238.
Larson, A. C. & von Dreele, R. B. (1994). *GSAS*. LANSCE, Los Alamos National Laboratory, NM, USA.
Marchivie, M., Guionneau, P., Howard, J. A. K., Goeta, A. E., Chastanet, G., Létard, J.-F. & Chasseau, D. (2002). *J. Am. Chem. Soc.* **124**, 194–195.
Money, V. A., Evans, I. R., Halcrow, M. A., Goeta, A. E. & Howard, J. A. K. (2003). *Chem. Commun.* pp. 158–159.
Money, V. A., Sánchez Costa, J., Marcén, S., Chastanet, G., Elna, K. J., Halcrow, M. A. & Létard, J.-F. (2002). Unpublished results.
Pawley, G. S. (1981). *J. Appl. Cryst.* **14**, 357–361.
Rietveld, H. (1969). *J. Appl. Cryst.* **2**, 65–71.
Visser, J. W. (1969). *J. Appl. Cryst.* **2**, 89–95.